scientific reports

Check for updates

OPEN

Elevated UBC9 expression and its oncogenic role in colorectal cancer progression and chemoresistance

Feng Li[1,8]✉, Yongmei Dai[2,8], Chenchen Tang[3,8], Lu Peng[4], Haijian Huang[1], Yuluo Chen[7], Yining Xu[5], Xuequn Chen[5,6]✉, Qingshui Wang[5]✉ & Yao Lin[5]✉

Colorectal cancer (CRC) is a highly prevalent and fatal malignancy, with incidence and mortality rates rising globally. While elevated UBC9 expression has been implicated in various cancers, its specific role in CRC remains poorly understood. This study aims to investigate the expression levels, prognostic significance, and functional roles of UBC9 in CRC. We assessed the expression and prognostic value of UBC9 mRNA and protein in colorectal cancer separately using multiple databases and immunohistochemical techniques. Additionally, in vitro functional assays and in vivo zebrafish tumor models were employed to elucidate the role of UBC9 in CRC cell proliferation, migration, invasion, and chemoresistance. UBC9 expression was significantly upregulated in CRC tissues. Elevated UBC9 levels were associated with poor prognosis in chemotherapy-treated CRC patients. Gene Set Enrichment Analysis revealed that pathways related to MYC targets, DNA repair, and oxidative stress response were enriched in groups with high UBC9 expression. Immune profiling indicated reduced infiltration of CD4+ memory-activated T cells and NK cells in tumors with elevated UBC9 levels. Functional assays demonstrated that UBC9 knockdown inhibited CRC cell proliferation, migration, and invasion, and sensitized cells to oxaliplatin, which was further validated using zebrafish xenograft models. UBC9 is crucial for CRC progression, genomic instability, and chemoresistance. It represents a potential prognostic biomarker and therapeutic target, particularly for enhancing chemotherapy efficacy in CRC patients.

Keywords Colorectal cancer, UBC9, SUMOylation, Prognosis, Chemoresistance

Colorectal cancer (CRC) ranks third in incidence and second in mortality among malignant tumors worldwide, and it is the leading cause of cancer death in men aged 20–49[1,2]. Globally, both the incidence and mortality rates of CRC are rising, with new cases and deaths projected to reach 3.2 million and 1.6 million, respectively, by 2040[3]. This trend underscores the urgent need for a deeper understanding and better management strategies to combat the increasing burden of CRC[4].

Post-translational modifications (PTMs) play crucial roles in regulating various biological processes[5]. Among them, SUMOylation is a significant PTM that influences DNA damage repair, nuclear transport, and signal transduction[6–8]. UBC9, the sole SUMO E2 conjugating enzyme, has attracted substantial attention due to its role in promoting cell proliferation in various cancers, including glioblastoma, osteosarcoma, and prostate cancer[9]. Elevated UBC9 expression is associated with poor prognosis in lung, breast, and pancreatic cancers. In chondrosarcoma, high UBC9 expression correlates with higher histological grading, while in MYC-amplified subtypes of pancreatic cancer, UBC9 expression is markedly increased, contributing to aggressive tumor behavior and lower survival rates[10–12]. However, the precise roles and mechanisms of UBC9 in CRC remain

[1]Department of Pathology, Shengli Clinical Medical College of Fujian Medical University and Fujian Provincial Hospital, Fuzhou University Affiliated Provincial Hospital, Fuzhou 350001, China. [2]Departments of Oncology, Shengli Clinical Medical College of Fujian Medical University and Fujian Provincial Hospital, Fuzhou University Affiliated Provincial Hospital, Fuzhou 350001, China. [3]Longyan First Hospital Affiliated to Fujian Medical University, Longyan 361000, China. [4]The School of Basic Medical Sciences, Fujian Medical University, Fuzhou 350001, China. [5]Fujian-Macao Science and Technology Cooperation Base of Traditional Chinese Medicine-Oriented Chronic Disease Prevention and Treatment, Innovation and Transformation Center, Fujian University of Traditional Chinese Medicine, Fuzhou 350001, China. [6]Rehabilitation Technology Innovation Center by Joint Collaboration of Ministry of Education and Fujian Province, Fujian University of Traditional Chinese Medicine, Fuzhou 350001, China. [7]Fujian Normal University, Fuzhou 350001, China. [8]These authors contributed equally: Feng Li, Yongmei Dai and Chenchen Tang. ✉email: lfeng0108@126.com; chenxq@fjtcm.edu.cn; wangqingshui@fjtcm.edu.cn; yaolin@fjtcm.edu.cn

poorly understood. Given the complexity and heterogeneity of CRC, elucidating the expression patterns and functional implications of UBC9 could provide invaluable insights into the disease's pathology and help identify potential therapeutic targets.

In this study, we investigate the expression and prognostic significance of UBE2I, the gene encoding UBC9, in CRC by utilizing multiple patient cohorts. We assess the impact of UBE2I expression on CRC patients' prognosis, particularly in the context of chemotherapy, and investigate the molecular pathways and clinical features associated with UBE2I. Additionally, we examine the functional roles of UBC9 in CRC cell proliferation, migration, invasion, and chemoresistance using both in vitro assays and an in vivo zebrafish tumor model. By elucidating the roles and implications of UBC9 in CRC, we aim to advance the understanding of CRC pathogenesis and progression, potentially paving the way for the development of more effective therapeutic interventions.

Methods

Clinical data collection and extraction

To gather the required data for our study, we extracted transcriptome RNA-sequencing data and associated clinical information for CRC from the TCGA database. Additionally, we obtained gene expression profiles along with clinical data from the GSE21510, GSE25071, GSE71187, GSE87211, and GSE106584 datasets available in the GEO database. We adhered to the same protocol for retrieving microarray gene expression data as described in our earlier research.

Patients and specimens

We collected a total of 100 surgical specimens from CRC patients at Fujian Provincial Hospital. Each case was pathologically confirmed by two pathologists, and all tissues were fixed in 10% neutral formalin and embedded in paraffin. The inclusion criteria were as follows: (1) Tumor lesions were surgically resected; (2) All CRC patients were sporadic cases; (3) Patients had not received radiotherapy, chemotherapy, or targeted therapy prior to surgery; (4) Pathological diagnosis was confirmed, and clinical data were complete. The exclusion criteria included: (1) Patients with other malignant tumors; (2) Patients who had received radiotherapy, chemotherapy, or targeted therapy before surgery; (3) Incomplete clinical pathological data. The clinical pathological information collected comprised of gender, age, tumor size, gross type, tumor location, vascular cancer embolus status, lymph node metastasis status, histological type, histological grade, TNM stage (according to the 8th edition of the TNM classification of malignant tumors by UICC/AJCC), tumor mutation status (KRAS, BRAF, NRAS mutations), overall survival (OS), and progression-free survival (PFS). The study was conducted with the approval of the Ethics Committee of Fujian Provincial Hospital and complied with the Helsinki Declaration. Written informed consent was obtained from all patients involved. Specimens were stored in the hospital database and utilized for research purposes.

IHC staining

Immunohistochemical (IHC) staining was performed to evaluate UBC9 protein levels in 100 colorectal cancer (CRC) tissues and their adjacent normal tissues. Sections (3 μm thick) from paraffin-embedded CRC and adjacent normal tissues were first deparaffinized with dimethylbenzene and then rehydrated. For antigen retrieval, sections were immersed in 0.01 mol/L sodium citrate buffer (pH 6.0) and autoclaved at 121 °C for 2 min. Endogenous peroxidase activity was blocked by incubating the sections in 3% hydrogen peroxide for 10 min at room temperature, followed by rinsing with PBS. To prevent non-specific binding, sections were treated with 10% goat serum (ZhongShan Biotechnology, China) for 30 min. After blocking, the sections were incubated overnight at 4 °C with a UBC9 antibody (ab75854, Abcam) diluted at 1:100. Following three washes with PBS, sections were incubated with an HRP-conjugated secondary antibody for 30 min at room temperature. The immunoreaction was visualized using diaminobenzidine solution, and counterstaining was performed with 20% hematoxylin, followed by dehydration.

Evaluation of immunostaining intensity

UBC9 positivity is determined by the presence of brownish-yellow granules in the cytoplasm/nucleus. Immunoreactivity was assessed using H-scores, which range from 0 to 300 and were calculated by multiplying the intensity of staining (0—no staining, 1+—weak staining, 2+-moderate staining, or 3+—strong staining) and the percentage of immunopositive cells (0–100). Based on H-score, expression of UBC9 was classified as low expression (H-score < 100) and high expression (H-score ≥ 100).

Analysis of immune environment

We utilized the CIBERSORT algorithm to assess the composition of immune cell types within tumor specimens based on gene expression profiles. The investigation focused on examining the relationship between UBE2I and the degree of immune cell infiltration into the tumors.

GSEA analysis

We downloaded the GSEA software from the official website (https://software.broadinstitute.org/gsea/index.jsp) and used hallmark gene sets from MSigDB as reference. CRC patients were classified into UBE2I-low and UBE2I-high expression groups. Each analysis was performed with 1000 iterations using the default weighted enrichment statistical method.

Cell culture
DLD-1 and HCT116 cell lines were sourced from the American Type Culture Collection (ATCC). These cells were cultured in RPMI-1640 medium supplemented with 10% fetal bovine serum and 1% penicillin–streptomycin, maintained in a humidified atmosphere with 5% CO_2 at 37 °C.

RNA isolation and analysis
Total RNA was extracted from DLD-1 and HCT116 cells using Trizol reagent (Invitrogen, California, USA). For reverse transcription, a kit from Takara was employed to synthesize cDNA from mRNA. RT-qPCR was performed to determine UBE2I mRNA expression levels, utilizing primers synthesized by Sangon Biotech (Shanghai, China). The primer sequences for UBE2I were: forward 5′-ACCATTATTTCACCCGAATGTGT-3′ and reverse 5′-CTCGGACCCTTTTCTCGTACT-3′. GAPDH served as the internal control with the following primer sequences: forward 5′-GCGGGGCTCTCCAGAACATCAT-3′ and reverse 5′-CCAGCCCCAGCGTC AAAGGTG-3′. Gene expression was quantified using the comparative $2^{-\Delta\Delta CT}$ method to determine relative mRNA levels.

UBC9-shRNA stable transfection
293 T cells were transfected with pLP1, pLP2, pLP/VSVG and UBC9-shRNAs. Supernatants containing the lentivirus were harvested after 48 h incubation and used to infect target cells. HCT116 and DLD-1 cells were selected with puromycin to establish stable cell lines. The sequences of UBC9 shRNA were 5′-TTGGCAGTAAA TCGTGTAGGCC-3′ (UBC9–shRNA1) and 5′-ATTTAGAAGTTCCTGTATTCCT-3′ (UBC9–shRNA2).

CCK-8 assay
To evaluate cell proliferation, DLD-1 and HCT116 cells were seeded at a density of 20,000 cells per well in 96-well plates and monitored at 24, 48, and 72-h intervals. At each time point, 10 µL of CCK-8 reagent was added to each well and incubated for four hours. Absorbance was then measured at 450 nm using a microplate spectrophotometer.

Invasion assay
For the invasion assay, DLD-1 and HCT116 cells were seeded onto insert membranes within invasion chambers using serum-free medium. The lower compartment was filled with RPMI-1640 medium supplemented with 10% FBS to promote cell migration. After 48 h, cells that had invaded through the membrane were fixed with methanol and stained with crystal violet. Non-invading cells were removed, and the invaded cells on the underside of the membrane were counted in six random fields for quantification.

Migration assay
To assess migration, scratch assays were performed on near-confluent layers of DLD-1 and HCT116 cells. After creating the wound, cell cultures were washed with PBS to remove debris and then incubated in serum-free medium to minimize the influence of growth factors on migration. Images of the wound area were captured 48 h post-scratch to measure the extent of wound healing.

Drug cytotoxicity assay
Drug cytotoxicity was evaluated using the CCK-8 assay. Cells were plated in a 96-well plate and treated with different concentrations of oxaliplatin for 48 h. After the treatment period, the medium was replaced with CCK-8 reagent. The cells were incubated with the reagent for two hours, and absorbance was subsequently measured at 450 nm using a microplate reader.

Zebrafish xenograft assay
Zebrafish were acquired from Fuzhou Bio-Service Biotechnology Co., Ltd. HCT116 cells, stained with the red-fluorescent lipophilic dye Dil (1,1′-dioctadecyl-3,3,3′,3′-tetramethylindocarbocyanine perchlorate) from Meilun Biotechnology (Dalian, China), using a 5 µM solution, were prepared for transplantation. Cells were meticulously injected into the yolk sac center or ventral yolk cavity of 2 days post-fertilization (2 dpf) zebrafish larvae using a precision microinjector. Each larva received approximately 200 labeled cells, with ten larvae included in each experimental group. To evaluate tumor cell proliferation within the zebrafish model, fluorescent imaging was performed at 2 h and 48 h post-transplantation. Metastatic progression was assessed by capturing images of tail fluorescence at 2 h and 24 h post-injection. This imaging process enabled the analysis of both localized tumor growth and the extent of metastatic spread within the experimental subjects. All zebrafish experiments are performed in accordance with the Animals (Scientific Procedures) Act 1986, and approved by the Fuzhou University Affiliated Provincial Hospital Animal Welfare and Ethical Review Body. The study is reported in accordance with ARRIVE guidelines.

Statistical analysis
Results are presented as mean ± standard deviation (SD). Pearson's correlation coefficient was utilized to assess statistical correlations. Two-way ANOVA was performed to analyze the CCK8 assay results. For survival analysis, hazard ratios (HR) and p-values were calculated using univariate Cox regression analysis. Kaplan–Meier survival curves were compared using log-rank tests. A p-value < 0.05 was considered statistically significant.

Results

Expression and prognostic analysis of UBE2I in colorectal cancer

In this study, we investigated the expression and prognostic significance of the UBC9 encoding gene UBE2I in CRC using several cohorts, including TCGA, GSE21510, GSE25071, GSE71187, and GSE87211. Our analysis showed a significant upregulation of UBE2I expression in CRC compared to adjacent normal tissues. This was observed in all cohorts (Fig. 1A, TCGA, $p < 0.001$; Fig. 1B, GSE21510, $p < 0.001$; Fig. 1C, GSE25071, $p < 0.01$; Fig. 1D, GSE71187, $p < 0.001$; Fig. 1E, GSE87211, $p < 0.001$). We further assessed the impact of UBE2I expression on the prognosis of CRC patients using the TCGA and GSE106584 cohorts. Survival analysis in the TCGA cohort did not show a significant association between UBE2I expression and prognosis (Fig. 1F, $p > 0.05$). However, in the GSE106584 cohort, which included patients who received chemotherapy, high UBE2I expression was significantly associated with poor prognosis in CRC patients (Fig. 1G, $p < 0.05$). These findings suggest that UBE2I is overexpressed in CRC and may serve as a potential prognostic marker, particularly in patients undergoing chemotherapy.

Correlation analysis of UBE2I with clinical features in colorectal cancer

Subsequently, we performed an in-depth analysis to investigate the correlation between UBE2I expression and various clinical features in colorectal cancer. Firstly, we examined the association between UBE2I expression and demographic factors, including age and gender. Our analysis revealed no significant differences in UBE2I expression across different age groups (Fig. 2A, $p > 0.05$) and between male and female patients (Fig. 2B, $p > 0.05$). This suggests that UBE2I expression is not influenced by these demographic characteristics in colorectal cancer. Furthermore, we investigated the relationship between UBE2I expression and specific clinical parameters, such as microsatellite status, T stage, and M stage. Our analysis indicated no significant variations in UBE2I expression among different microsatellite statuses (Fig. 2C, $p > 0.05$) and T stages (Fig. 2D, $p > 0.05$). Similarly, there were no notable differences in UBE2I expression based on M stage (Fig. 2E, $p > 0.05$). However, when considering

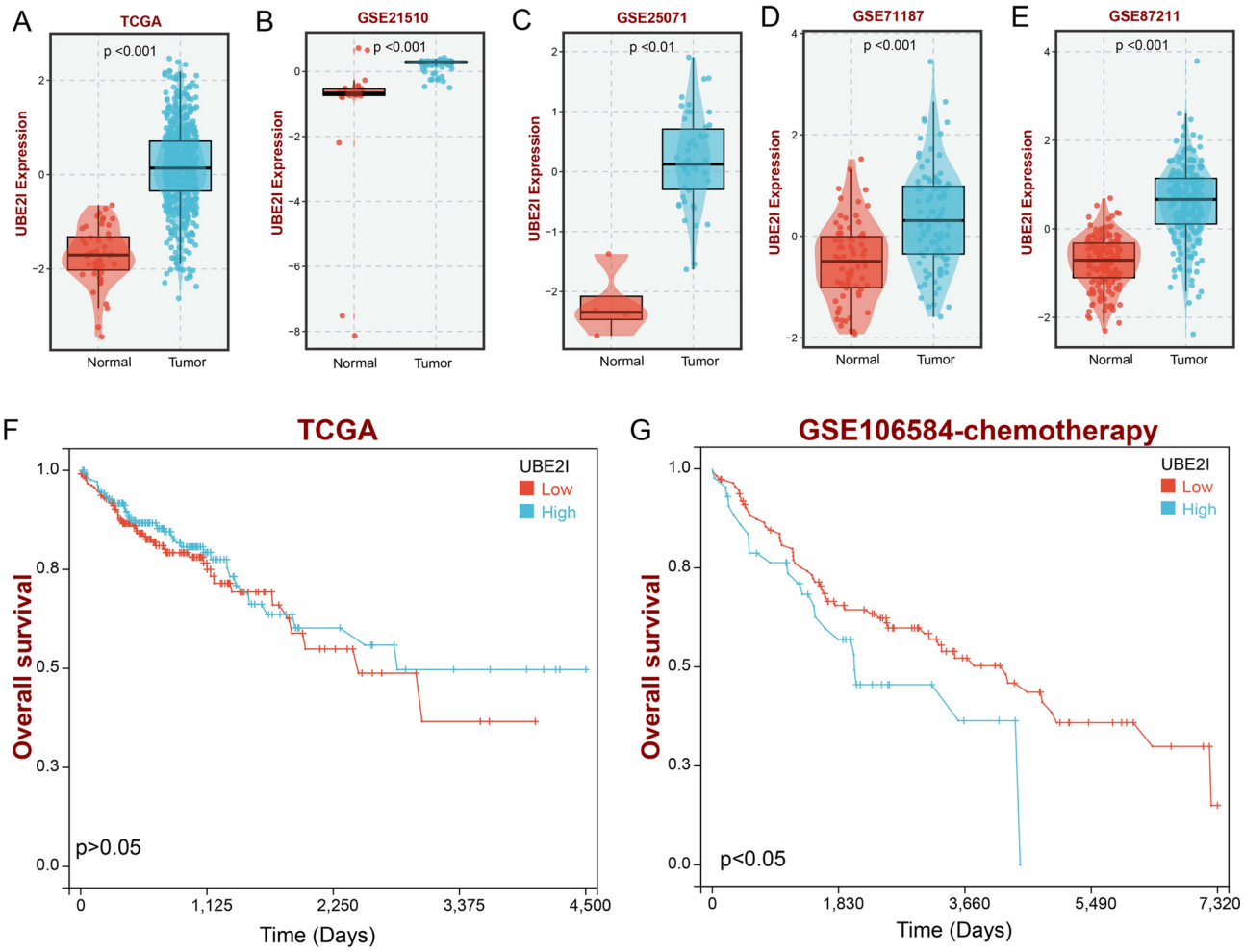

Fig. 1. Expression and prognostic analysis of UBE2I in colorectal cancer. (**A**–**E**) Expression of UBE2I in colorectal cancer and adjacent normal tissues in the (**A**) TCGA, (**B**) GSE21516, (**C**) GSE25071, (**D**) GSE71187, and (**E**) GSE87211 datasets; (**F** and **G**) Prognostic analysis of UBE2I in the (**F**) TCGA and (**G**) GSE106584 datasets.

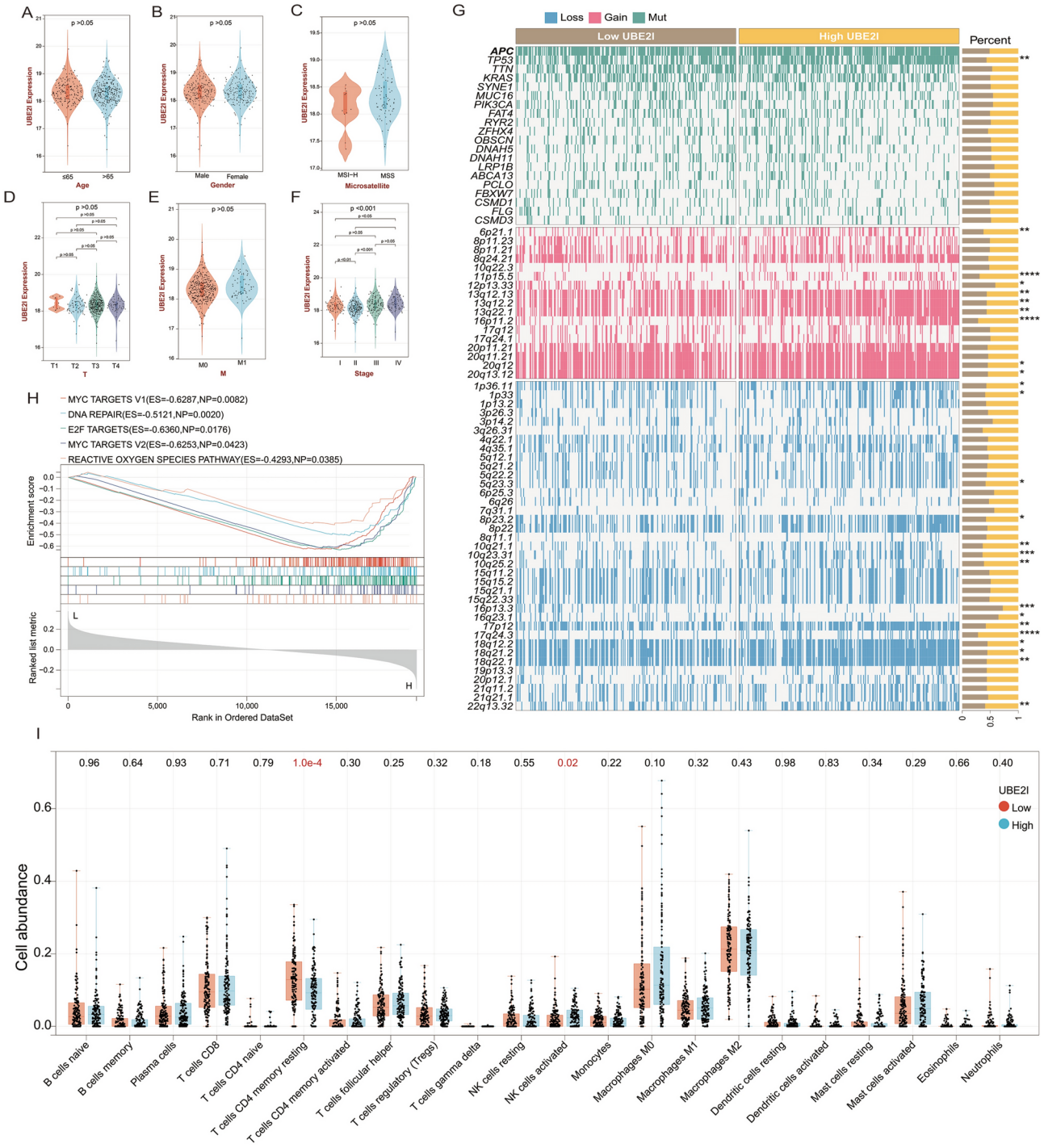

Fig. 2. Correlation analysis of UBE2I with clinical characteristics of colorectal cancer. (**A**–**F**) Correlation analysis of UBE2I expression with clinical characteristics of colorectal cancer patients, including (**A**) age, (**B**) gender, (**C**) microsatellites, (**D**) TV stage, (**E**) M stage, and (**F**) overall stage. (**G**) Analysis of gene variation differences between the UBE2I-Low and UBE2I-High groups; (**H**) GSEA analysis of signaling pathways enriched in the UBE2I high expression group; (**I**) Correlation analysis of UBE2I expression with immune cell infiltration.

the stage subgroup, we observed a significant difference in UBE2I expression (Fig. 2F, $p < 0.001$), suggesting its potential involvement in the progression of colorectal cancer.

To gain further insights into the underlying molecular alterations associated with UBE2I expression, we conducted a genomic alteration analysis. Intriguingly, our results demonstrated a higher TP53 mutation rate in the UBE2I high-expression group (Fig. 2G). This finding suggests a potential interplay between UBE2I and TP53, highlighting UBE2I's role in genomic instability and tumorigenesis in colorectal cancer.

Additionally, we performed Gene Set Enrichment Analysis (GSEA) to explore the functional implications of UBE2I expression. The analysis revealed significant enrichment of several pathways in the UBE2I high-expression group, including MYC targets V1, DNA repair, E2F targets, MYC targets V2, and Reactive oxygen species pathway (Fig. 2H). These findings suggest that UBE2I may influence critical cellular processes involved in proliferation, DNA repair, and oxidative stress response, contributing to the aggressive phenotype observed in colorectal cancer.

Moreover, we investigated the relationship between UBE2I expression and immune cell infiltration within the tumor microenvironment. Notably, our results demonstrated significantly higher infiltration of T cells CD4 memory activated and NK cells activated in the UBE2I low-expression group compared to the UBE2I high-expression group (Fig. 2I). These findings suggest a potential immunomodulatory role of UBE2I in shaping the immune landscape of colorectal tumors.

Expression and prognostic significance of UBC9 protein in colorectal cancer

Next, we evaluated the expression of UBC9 in cancerous and adjacent non-cancerous tissues from 100 colorectal cancer patients using immunohistochemistry. Based on UBC9 protein expression, patients were categorized into high and low expression groups. We found that UBC9 was highly expressed in 74% (74/100) of colorectal cancer tissues and lowly expressed in 26% (26/100). In contrast, adjacent non-cancerous tissues exhibited 19% (19/100) high expression and 81% (81/100) low expression (Fig. 3A,B). Immunohistochemical scoring further confirmed that UBC9 protein levels were significantly elevated in colorectal cancer tissues compared to adjacent non-cancerous tissues (Fig. 3C). Furthermore, we observed that UBC9 protein expression is significantly elevated in tissues from colorectal cancer patients with KRAS mutations when compared to those with KRAS wild-type (Fig. 3D).

Statistical analysis revealed that high UBC9 expression was significantly associated with older age, lymph node metastasis, and advanced TNM stage. However, it did not show significant associations with gender, tumor size, gross type, histological type, vascular invasion, or common tumor mutations (KRAS, BRAF, NRAS) (Table 1). Kaplan–Meier survival analysis demonstrated that patients with low UBC9 expression had significantly longer overall survival (OS) and disease-free survival (DFS) compared to those with high UBC9 expression (Fig. 3E,F).

Univariate Cox regression analysis identified older age, higher histological grade, presence of vascular invasion, lymph node metastasis, advanced TNM stage, and high UBC9 expression as prognostic factors for poorer OS in CRC patients. Gender, tumor size, location, gross type, histological type, and common driver mutations did not show prognostic significance for OS (Fig. 3G). Similarly, univariate analysis indicated that older age, higher histological grade, presence of vascular invasion, high UBC9 expression, lymph node metastasis, and advanced TNM stage were prognostic factors for shorter DFS in CRC patients. Gender, tumor characteristics, and common driver mutations were not prognostic for DFS (Fig. 3H).

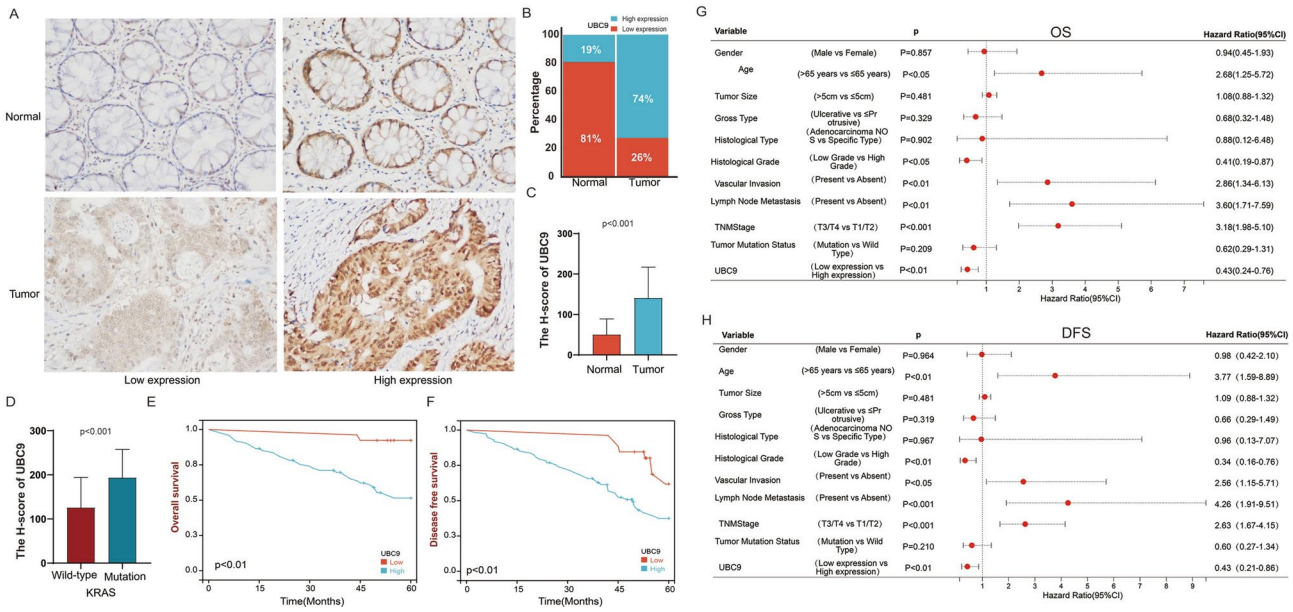

Fig. 3. Expression and prognostic analysis of UBC9 in colorectal cancer. (**A**) Representative images of UBC9 expression in 100 colorectal cancer samples; (**B**) Histogram showing the expression of UBC9 in colorectal cancer tissues versus adjacent normal tissues; (**C**) Immunohistochemical scoring of UBC9 protein in colorectal cancer and adjacent normal tissues; (**D**) Analysis of UBC9 Protein Expression in Tissues from CRC Patients with KRAS Mutations and KRAS Wild-Type; (**E** and **F**) Analysis of (**E**) overall survival and (**F**) disease-free survival based on UBC9 protein levels in 100 colorectal cancer patients; (**G** and **H**) Cox univariate survival analysis of (**G**) overall survival and (**H**) disease-free survival in 100 colorectal cancer patients.

Clinical pathological features	UBC9 high expression	UBC9 low expression	P value
Gender			0.387
Male	28	27	
Female	19	26	
Age			0.006
≤65years	18	35	
>65years	29	18	
Tumor size			0.181
≤5cm	39	38	
>5cm	8	15	
Gross type			0.504
Ulcerative	28	35	
Protrusive	19	18	
Histological type			1.000
Adenocarcinoma NOS	45	51	
Specific type	2	2	
Histological grade			0.483
Low grade	39	41	
High grade	8	12	
Vascular invasion			0.251
Present	24	21	
Absent	23	32	
Lymph node metastasis			0.020
Present	23	14	
Absent	24	39	
TNMStage			0.019
T1/T2	21	36	
T3/T4	26	17	
Tumor mutation status			0.598
KRAS mutation	32	15	
BRAF mutation	2	3	
NRAS mutation	1	4	
Wild type	20	23	

Table 1. Relationship between UBC9 protein expression and clinicopathological characteristics in patients with colorectal cancer.

Knockdown of UBC9 inhibits the proliferation and metastasis of colorectal cancer cells

To further elucidate the impact of UBC9 on the function of colorectal cancer cells, we established stable UBC9 knockdown cells in HCT116 (Fig. 4A). We then evaluated the effects of UBC9 knockdown on the proliferation, migration, and invasion abilities of HCT116 cells using CCK8 assays, wound healing assays, and Transwell assays, respectively. The experimental results showed that UBC9 knockdown significantly inhibited the proliferation (Fig. 4B), migration (Fig. 4C), and invasion (Fig. 4D) abilities of HCT116 cells. Subsequently, we also established stable UBC9 knockdown cells in DLD-1 cells (Fig. 5A). The experimental results demonstrated that UBC9 knockdown significantly inhibited the proliferation (Fig. 5B), migration (Fig. 5C), and invasion (Fig. 5D) abilities of DLD-1 cells as well.

To explore the biological function of UBC9 in vivo, we utilized a zebrafish tumor xenograft model to verify the proliferation and migration abilities of HCT116 cells. Zebrafish, being an ideal vertebrate model, have highly conserved signaling pathways with human diseases, making them suitable for evaluating the roles and functions of human genes. Additionally, their transparent bodies allow direct observation of internal organs.

As shown in Fig. 6A, HCT116 tumor cells were injected into the yolk sac of 48 hpf zebrafish embryos. Two hours post-injection, there was no significant difference in fluorescence area between the NC group and UBC9-shRNAs group; however, at 48 h post-injection, the fluorescence area of tumor cells in the UBC9-shRNAs group was significantly reduced compared to the NC group, suggesting that UBC9 knockdown may inhibit the proliferation of HCT116 cells in zebrafish.

As illustrated in Fig. 6B, HCT116 tumor cells were injected into the ventral yolk cavity of 48 hpf zebrafish embryos. Two hours post-injection, there was no significant difference in fluorescence area in the tail region of tumor cells between the NC group and UBC9-shRNAs group. However, 24 h post-transplantation, the fluorescence area of tumor cells in the tail region of the UBC9-shRNAs group was significantly reduced compared to the NC group, indicating that UBC9 knockdown may inhibit the metastasis of HCT116 cells in zebrafish.

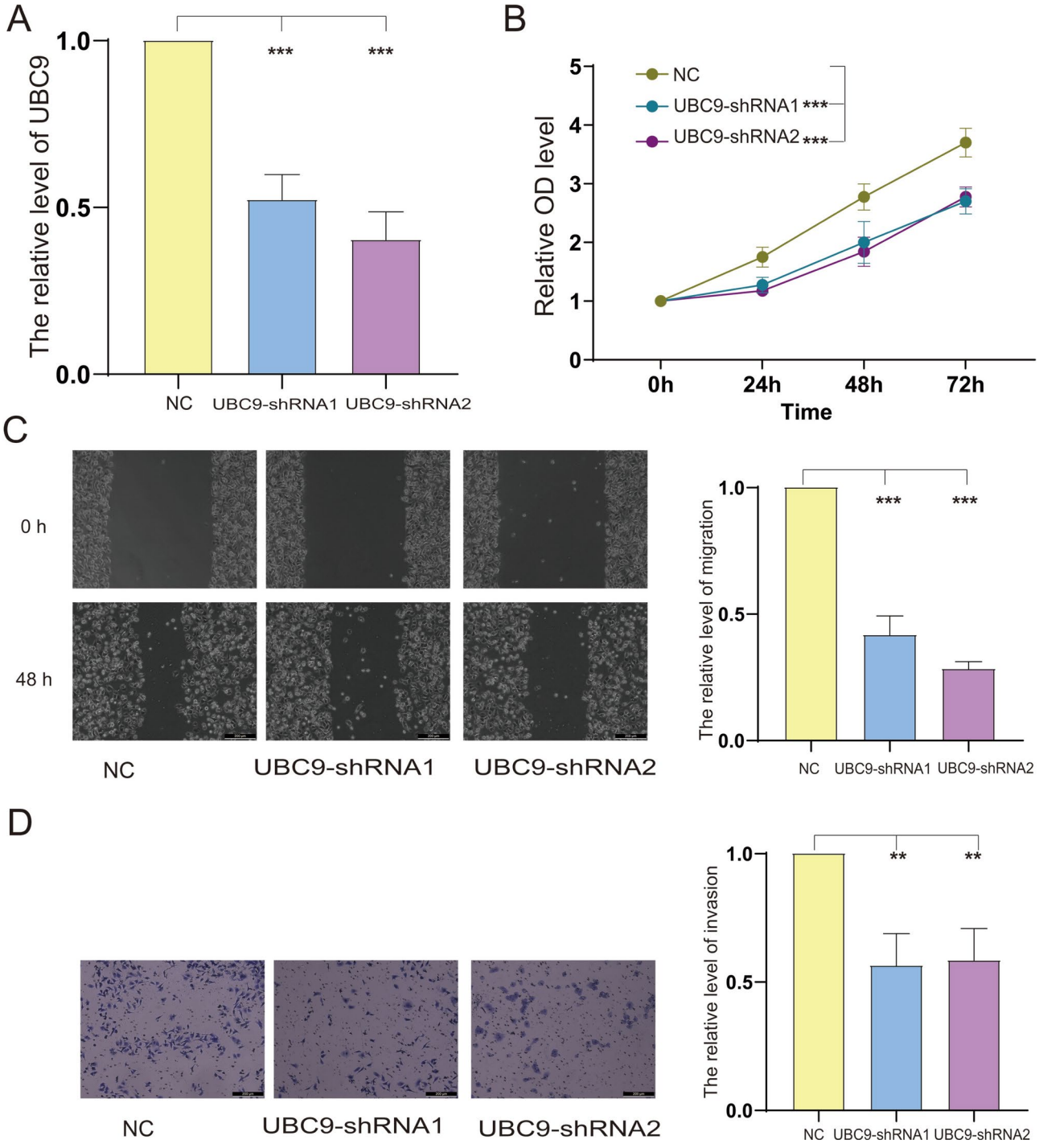

Fig. 4. Knockdown of UBC9 inhibits proliferation, migration, and invasion of HCT116 cells. (**A**) RT-PCR analysis of UBE2I expression; (**B**) CCK8 assay to assess the effect of UBC9 knockdown on HCT116 cell proliferation; (**C**) Wound healing assay to evaluate the impact of UBC9 knockdown on HCT116 cell migration; (**D**) Transwell assay to determine the effect of UBC9 knockdown on HCT116 cell invasion. $^{**}p < 0.01$; $^{***}p < 0.001$.

Knockdown of UBC9 enhances sensitivity to Oxaliplatin in colorectal cancer cells

We have identified that UBE2I holds prognostic significance for colorectal cancer patients undergoing chemotherapy (Fig. 1G). Building on this finding, we investigated the relationship between UBC9 and the sensitivity of colorectal cancer cells to oxaliplatin. Our drug cytotoxicity assays demonstrated that silencing UBC9 increases the sensitivity of HCT116 and DLD-1 cell lines to oxaliplatin, as evidenced by a reduction in the IC50 concentration of the drug (Fig. 7).

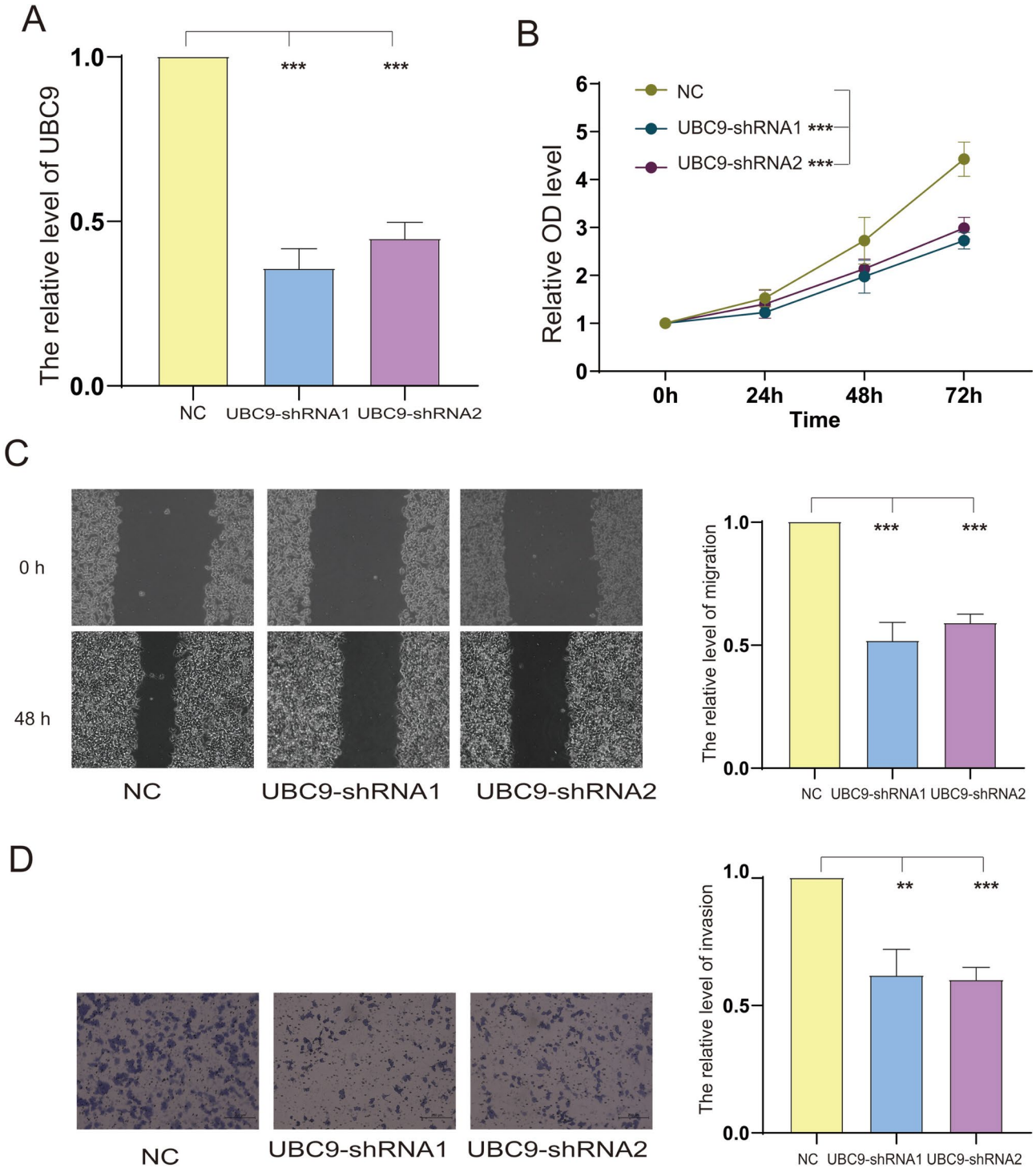

Fig. 5. Knockdown of UBC9 inhibits proliferation, migration, and invasion of DLD-1 cells. (**A**) RT-PCR analysis of UBE2I expression; (**B**) CCK8 assay to assess the effect of UBC9 knockdown on DLD-1 cell proliferation; (**C**) Wound healing assay to evaluate the impact of UBC9 knockdown on DLD-1 cell migration; (**D**) Transwell assay to determine the effect of UBC9 knockdown on DLD-1 cell invasion. $^{**}p < 0.01$; $^{***}p < 0.001$.

Discussion

CRC remains one of the most prevalent and lethal malignancies affecting the digestive system. According to the 2022 cancer report, CRC is the second leading cause of cancer incidence and the fifth leading cause of cancer-related mortality in China, with 592,232 new cases and 309,114 deaths reported[13]. These numbers represent a significant increase compared to 2020, which saw 555,477 new cases and 286,162 deaths, underscoring an urgent

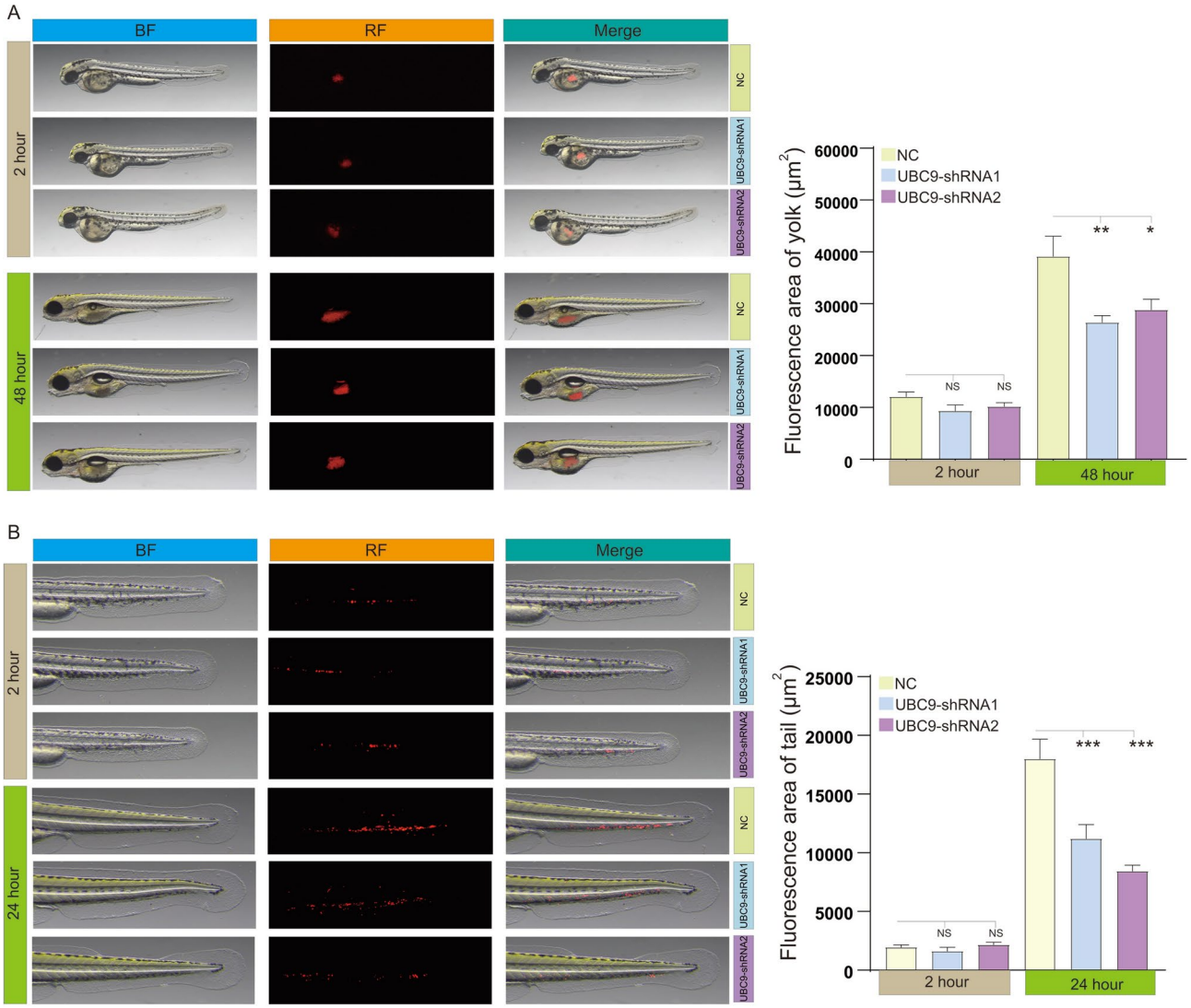

Fig. 6. Knockdown of UBC9 inhibits proliferation and metastasis of colorectal cancer cells in Zebrafish. (**A**) Effect of UBC9 knockdown on the proliferation of colorectal cancer cells in zebrafish; (**B**) Effect of UBC9 knockdown on the metastasis of colorectal cancer cells in zebrafish. ns, $p > 0.05$; *$p < 0.05$; **$p < 0.01$; ***$p < 0.001$.

need to better understand and address the factors driving CRC. Chromosomal instability is a major contributing factor to the development and progression of CRC, characterized by the loss of tumor suppressor gene loci, chromosomal rearrangements, and mutations in key genes such as KRAS, BRAF, PIK3CA, and TP53[14–16]. While advancements in therapeutic approaches and patient management have led to some improvements in overall survival rates, the prognosis for advanced CRC, particularly stage IV, remains poor, with a 5-year survival rate of around 20%[17]. This scenario highlights the critical need for novel and effective therapeutic strategies to improve survival outcomes for CRC patients.

SUMOylation is an essential post-translational modification (PTM) involved in a myriad of biological processes including DNA damage repair, nuclear transport, and cell signal transduction[18]. UBC9 is the sole SUMO E2 conjugating enzyme, and its overexpression has been shown to promote the proliferation of glioblastoma, osteosarcoma, and prostate cancer cells[19]. In lung, breast, and pancreatic cancers, high UBC9 expression is associated with poor prognosis[20]. Elevated UBC9 expression in chondrosarcoma correlates with higher histological grading[21]. Specifically, UBC9 expression is markedly higher in MYC-amplified subtypes of pancreatic cancer, which are more aggressive and associated with lower survival rates, accounting for approximately 12% of pancreatic cancer cases[22]. NSUN2 is the primary 5-methylcytosine (m5C) methyltransferase in mammals, and it regulates cell proliferation and metastasis by promoting m5C modification of target genes within the nucleus[23]. UBC9 stabilizes the NSUN2 protein and facilitates its entry into the nucleus to modify target proteins, thereby promoting the proliferation and metastasis of gastric cancer cells[24]. This study primarily focuses on the expression and functional analysis of UBC9 in colorectal cancer[25].

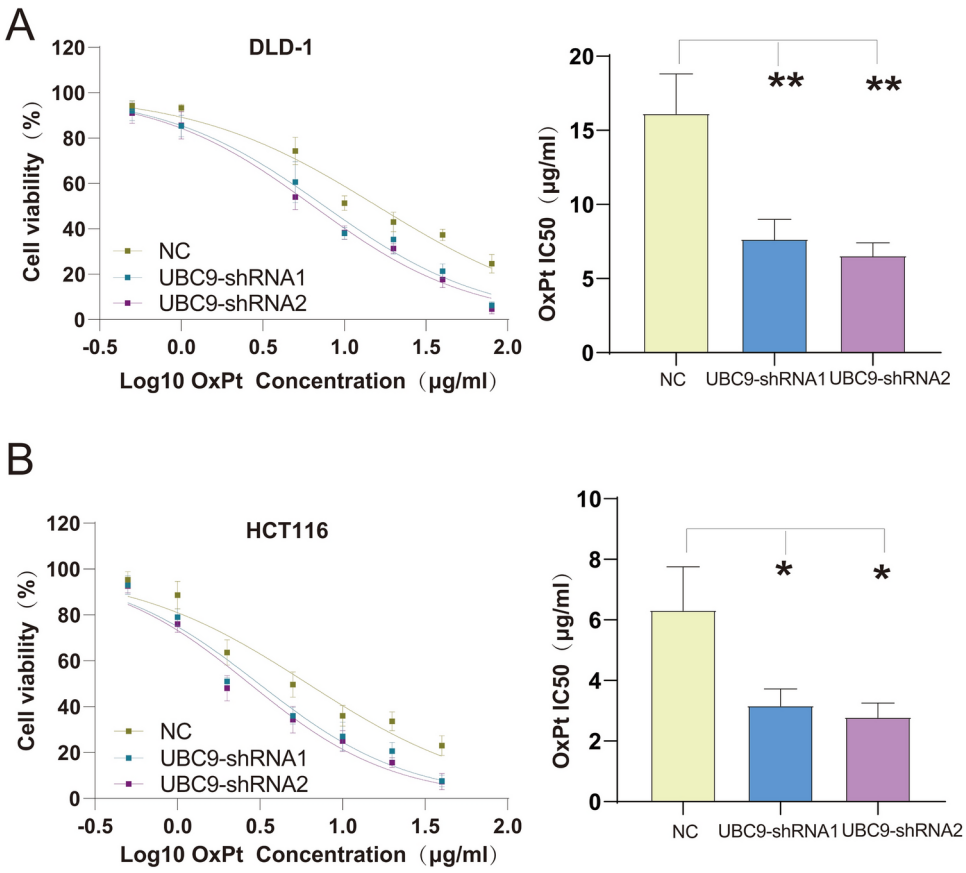

Fig. 7. Effect of UBC9 knockdown on Oxaliplatin resistance in colorectal cancer cells. (**A** and **B**) Effect of UBC9 knockdown on oxaliplatin resistance in (**A**) DLD-1 and (**B**) HCT116 cells. *p < 0.05; **p < 0.01.

Our findings elucidate the critical and multifaceted role of UBE2I (the gene encoding UBC9) in CRC, highlighting its expression, prognostic value, and functional implications. We observed that UBE2I is significantly upregulated in CRC tissues compared to adjacent normal tissues across multiple cohorts, suggesting its potential role as an oncogene. Moreover, the prognostic value of UBE2I appears to be context-dependent, with particularly unfavorable prognostic implications in patients undergoing chemotherapy, as demonstrated by the GSE106584 cohort.

Recent studies have indicated that UBC9, an E2 conjugating enzyme involved in the SUMOylation pathway, participates in various cellular processes, including transcriptional regulation, DNA repair, and signal transduction. The observed association between high UBE2I expression and increased TP53 mutation rates underscores the critical interplay between SUMOylation and genomic stability. TP53, a well-established tumor suppressor gene, plays a crucial role in maintaining genomic integrity. Mutation in TP53 is one of the most common genetic alterations in CRC[26], and the correlation with UBE2I expression suggests that aberrant SUMOylation may promote genomic instability and oncogenesis in CRC.

Our GSEA further supports this hypothesis, indicating that high UBE2I expression enriches pathways related to MYC targets, DNA repair, E2F targets, and reactive oxygen species (ROS) response. The enrichment of MYC targets V1 and V2 suggests that UBE2I might be facilitating MYC-driven transcriptional programs, which are known to promote cell proliferation and tumor growth. Additionally, the significant enrichment of DNA repair pathways implies that UBE2I could be modulating the repair mechanisms, potentially contributing to the survival of cancer cells under genotoxic stress. The association with the ROS pathway indicates a role for UBE2I in managing oxidative stress, which is a known contributor to cancer progression and chemoresistance.

Research indicates that UBC9 is essential for KRAS-driven transformation, as its depletion suppresses the growth of KRAS mutant colorectal cancer cells both in vitro and in vivo. Elevated SUMOylation of specific proteins, such as KAP1, CHD1, and EIF3L, contributes to the aggressive phenotype of KRAS mutant cells, highlighting UBC9 as a promising therapeutic target for treating KRAS mutant colorectal cancer[25]. Consequently, we conducted an analysis of UBC9 expression in tissues from colorectal cancer patients with KRAS mutations and those with KRAS wild-type. The results indicated that UBC9 expression is significantly elevated in tissues from KRAS-mutated colorectal cancer compared to those with KRAS wild-type. These findings suggest that targeting UBC9 may provide a novel approach to inhibit the progression of KRAS-driven colorectal cancer.

Moreover, our study also unveiled significant differences in immune cell infiltration between low and high UBE2I expression groups within the tumor microenvironment. Specifically, we found higher infiltration of CD4+ memory activated T cells and activated NK cells in the low UBE2I expression group. This finding

suggests that UBE2I may play an immunomodulatory role, potentially contributing to an immune-suppressive microenvironment that facilitates tumor progression. Activated T cells and NK cells are critical components of the anti-tumor immune response, and their reduced presence in high UBE2I expressing tumors may partially explain the poor prognosis observed in these patients. This immunosuppressive milieu could also provide insights into the observed chemotherapy resistance, as effective responses to chemotherapy are often contingent on a robust immune response.

In our functional assays, the knockdown of UBC9 in CRC cell lines significantly inhibited cell proliferation, migration, and invasion, indicating its role in driving the aggressive phenotype of CRC cells. Additionally, the in vivo zebrafish tumor xenograft model corroborated these findings, demonstrating that UBC9 knockdown impairs both proliferation and metastasis of CRC cells. These functional insights provide a strong rationale for targeting UBC9 as a therapeutic strategy in CRC. Notably, our results align with emerging evidence suggesting the multifaceted regulatory potential of UBC9. Previous research has shown that down-regulation of UBC9 expression can induce cell apoptosis and promote cellular quiescence by inhibiting the NF-κB signaling pathway in hepatic stellate cells[27]. Moreover, the potential significance of our findings is underscored by existing literature highlighting the cancer-promoting role of NF-κB signaling in the tumor microenvironment[28], where activation in stromal myofibroblasts correlates positively with the transformation of normal stroma into a cancer-supporting phenotype.

Oxaliplatin, as a DNA intercalating agent, induces DNA damage and causes DNA strand breaks, thereby activating apoptotic signaling pathways in cancer cells. It is the first platinum-based drug proven to have antitumor activity against colorectal cancer. Unfortunately, resistance to oxaliplatin leads to treatment failure, posing a significant challenge in the clinical treatment of colorectal cancer patients. Our investigation into the sensitivity of CRC cells to oxaliplatin revealed that silencing UBC9 enhances the cytotoxic effects of the chemotherapeutic drug. This finding is particularly relevant in the context of our earlier observation that high UBC9 expression correlates with poor prognosis in chemotherapy-treated patients. By modulating UBC9 expression, it might be possible to sensitize CRC tumors to chemotherapy, thereby improving clinical outcomes.

Conclusion

In conclusion, our study elucidates the pivotal role of UBC9 in CRC, highlighting its contributions to tumor progression, genomic instability, immunomodulation, and chemoresistance. These findings suggest that UBC9 could serve as a valuable biomarker and therapeutic target, particularly for enhancing the efficacy of chemotherapy in CRC patients.

Data availability

The datasets used to support the conclusion of this study were collected from publicly available databases including Cancer Genome Atlas database (https://portal.gdc.cancer.gov/) and Gene Expression Omnibus database (https://www.ncbi.nlm.nih.gov/geo/).

Received: 9 July 2024; Accepted: 10 March 2025
Published online: 17 March 2025

References

1. Li, J., Ma, X., Chakravarti, D., Shalapour, S. & Depinho, R. A. Genetic and biological hallmarks of colorectal cancer. *Genes Dev.* **35**, 787–820 (2021).
2. Eng, C. et al. A comprehensive framework for early-onset colorectal cancer research. *Lancet Oncol.* **23**, e116–e128 (2022).
3. Yan, H., Talty, R. & Johnson, C. H. Targeting ferroptosis to treat colorectal cancer. *Trends Cell Biol.* **33**, 185–188 (2023).
4. Messersmith, W. A. NCCN Guidelines updates: Management of metastatic colorectal cancer. *J. Natl. Compr. Canc. Netw.* **17**, 599–601 (2019).
5. Spaander, M. C. et al. Young-onset colorectal cancer. *Nat. Rev. Dis. Primers* **9**, 22 (2023).
6. Sheng, Z., Zhu, J., Deng, Y. N., Gao, S. & Liang, S. SUMOylation modification-mediated cell death. *Open Biol.* **11**, 210050 (2021).
7. Han, Z. J., Feng, Y. H., Gu, B. H., Li, Y. M. & Chen, H. The post-translational modification, SUMOylation, and cancer (Review). *Int. J. Oncol.* **52**, 1081–1094 (2018).
8. Demel, U. M. et al. Activated SUMOylation restricts MHC class I antigen presentation to confer immune evasion in cancer. *J. Clin. Invest.* **132**, 66 (2022).
9. Xiao, J. et al. UBC9 deficiency enhances immunostimulatory macrophage activation and subsequent antitumor T cell response in prostate cancer. *J Clin Invest* **133**, 66 (2023).
10. Mattoscio, D. et al. Autophagy regulates UBC9 levels during viral-mediated tumorigenesis. *PLoS Pathog.* **13**, e1006262 (2017).
11. Wang, L. & Ji, S. Inhibition of Ubc9-induced CRMP2 SUMOylation disrupts glioblastoma cell proliferation. *J. Mol. Neurosci.* **69**, 391–398 (2019).
12. Klug, H. et al. Ubc9 sumoylation controls SUMO chain formation and meiotic synapsis in Saccharomyces cerevisiae. *Mol. Cell.* **50**, 625–636 (2013).
13. White, M. T. & Sears, C. L. The microbial landscape of colorectal cancer. *Nat. Rev. Microbiol.* **22**, 240–254 (2024).
14. Mármol, I., Sánchez-De-Diego, C., Pradilla Dieste, A., Cerrada, E. & Rodriguez Yoldi, M. J. Colorectal Carcinoma: A General Overview and Future Perspectives in Colorectal Cancer. *Int. J. Mol. Sci.* **18**, 66 (2017).
15. Müller, M. F., Ibrahim, A. E. & Arends, M. J. Molecular pathological classification of colorectal cancer. *Virchows Arch.* **469**, 125–134 (2016).
16. Chen, B. et al. The long noncoding RNA CCAT2 induces chromosomal instability through BOP1-AURKB signaling. *Gastroenterology.* **159**, 2146.e33-2162.e33 (2020).
17. Harada, S. & Morlote, D. Molecular pathology of colorectal cancer. *Adv. Anat. Pathol.* **27**, 20–26 (2020).
18. Liu, S. et al. Sumoylation as an emerging target in therapeutics against cancer. *Curr. Pharm. Des.* **26**, 4764–4776 (2020).
19. Sabatini, M. E. et al. The UBC9/SUMO pathway affects E-cadherin cleavage in HPV-positive head and neck cancer. *Front. Mol. Biosci.* **9**, 940449 (2022).
20. Diao, X. et al. SUMOylation-triggered ALIX activation modulates extracellular vesicles circTLCD4-RWDD3 to promote lymphatic metastasis of non-small cell lung cancer. *Signal Transduct. Target Ther.* **8**, 426 (2023).

21. Zhu, S., Sachdeva, M., Wu, F., Lu, Z. & Mo, Y. Y. Ubc9 promotes breast cell invasion and metastasis in a sumoylation-independent manner. *Oncogene* **29**, 1763–1772 (2010).
22. Biederstädt, A. et al. SUMO pathway inhibition targets an aggressive pancreatic cancer subtype. *Gut* **69**, 1472–1482 (2020).
23. Feng, J. et al. NSUN2-mediated m5C modification of HBV RNA positively regulates HBV replication. *PLoS Pathog.* **19**, e1011808 (2023).
24. Hu, Y. et al. NSUN2 modified by SUMO-2/3 promotes gastric cancer progression and regulates mRNA m5C methylation. *Cell Death Dis.* **12**, 842 (2021).
25. Yu, B. et al. Oncogenesis driven by the Ras/Raf pathway requires the SUMO E2 ligase Ubc9. *Proc. Natl. Acad. Sci. USA* **112**, E1724–E1733 (2015).
26. Liebl, M. C. & Hofmann, T. G. The role of p53 signaling in colorectal cancer. *Cancers* **13**, 66 (2021).
27. Fang, S. et al. Downregulation of UBC9 promotes apoptosis of activated human LX-2 hepatic stellate cells by suppressing the canonical NF-κB signaling pathway. *PLoS ONE* **12**, e0174374 (2017).
28. Vandoros, G. P. et al. PPAR-gamma is expressed and NF-kB pathway is activated and correlates positively with COX-2 expression in stromal myofibroblasts surrounding colon adenocarcinomas. *J. Cancer Res. Clin. Oncol.* **132**, 76–84 (2006).

Author contributions
Feng Li, Yongmei Dai, Chenchen Tang carried out the bioinformatic analyses. Lu Peng, Haijian Huang, Yuluo Chen, Yining Xu conducted the experiments. Xuequn Chen, Qingshui Wang, Yao Lin supervised the work and wrote the manuscript.

Funding
This research was funded by the Natural Science Foundation of Fujian Provice (2022J011015 and 2022J01173), Rehabilitation technology innovation center by joint collaboration of ministry of education and Fujian province, Fujian University of Traditional Chinese Medicine (X2022009-xietong), and Fujian University of Traditional Chinese Medicine (X2023022).

Declarations

Competing interests
The authors declare no competing interests.

Ethics approval and consent to participate
The study was approved by the Research Ethics Committee of Fujian Provincial Hospital and complied with the Helsinki Declaration. The patients/participants provided their written informed consent to participate in this study.

Additional information
Correspondence and requests for materials should be addressed to F.L., X.C., Q.W. or Y.L.